Colloids and Surfaces A 580 (2019) 123791

Contents lists available at ScienceDirect

Colloids and Surfaces A

journal homepage: www.elsevier.com/locate/colsurfa

Evaluation of cellular uptake mechanisms for AuNP-collagen-Avemar nanocarrier on transformed and non-transformed cell lines

Huey-Shan Hung[a,b], Da-Tian Bau[a,c,d], Chun-An Yeh[a], Mei-Lang Kung[e,*]

[a] Graduate Institute of Biomedical Science, China Medical University, Taichung, Taiwan
[b] Translational Medicine Research, China Medical University Hospital, Taichung, Taiwan
[c] Terry Fox Cancer Research Laboratory, China Medical University Hospital, Taichung, Taiwan
[d] Department of Bioinformatics and Medical Engineering, Asia University, Taichung, Taiwan
[e] Department of Chemistry, National Sun Yat-Sen University, Kaohsiung, Taiwan

GRAPHICAL ABSTRACT

Schematic diagram illustrated that AuNP-Col-Ave-mediated cellular uptake mechanisms and cell fates in both transform and non-transformed cell lines.

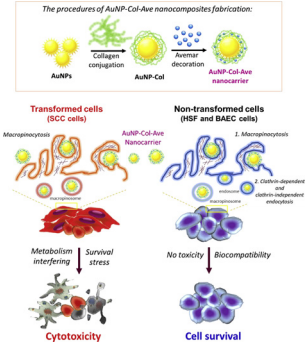

ARTICLE INFO

Keywords:
Nutrition therapy
Avemar
AuNP-collagen-Avemar nanocarrier
Endocytosis

ABSTRACT

Goldnanoparticles (AuNPs) have well applied in imaging and carriers of drugs and/or biomolecules for diseases and cancers therapeutics, due to their tunable physicochemical properties, easy functionalized with biomolecules and biocompatibility. AuNPs conjugated with biopolymer such as collagen has been demonstrated that increased the cell proliferation, migration and cell differentiation. Avemar (Ave) is a nutraceutical from natural components and dietary supplement for healthcare of tumor related anorexia/cachexia. Moreover, Ave has revealed the excellent bio-efficacy of anti-proliferation, cell cycle disturbing and apoptosis induction in numerous types of tumor cells in *in vivo* and *in vitro*. However, the effects of Ave on cellular uptake mechanisms still unclear. In this study, we fabricate the Ave-deposited AuNP-collagen nanocarrier (AuNP-Col-Ave) and investigate their endocytic mechanisms in transformed SCC oral cancer cells and non-transformed BAEC and HSF cell lines. By using DLS assay, Ave-deposited AuNP-Col have shown a particle size of 303 ± 35.2 nm. Both UV–vis absorption assay and FTIR spectrum analysis were also demonstrated that the Ave conjugated onto AuNP-Col. Further, both MTT assay and Calcein AM assay were revealed that AuNP-Col-Ave induced a significant cytotoxicity in cancerous SCC cells and showed nontoxicity and biocompatibility for non-transformed BAEC and HFS cells. In addition, AuNP-Col-Ave has showed an excellent uptake capacity in all these cell lines as compared to AuNP-Col group. Further uptake mechanisms analysis demonstrated that the macropinocytosis seems to be the favorite endocytic mechanism during AuNP-Col-Ave internalized into these transformed and

* Corresponding author at: Department of Chemistry, National Sun Yat-sen University, Kaohsiung, 80424, Taiwan.
E-mail address: kungmeilang@gmail.com (M.-L. Kung).

https://doi.org/10.1016/j.colsurfa.2019.123791
Received 14 July 2019; Received in revised form 10 August 2019; Accepted 11 August 2019
Available online 13 August 2019
0927-7757/

non-transformed cell lines. Altogether, this study is first validating the endocytic mechanisms of AuNP-Col-Ave in transformed and non-transformed cell lines. Our findings will provide a novel insight for endocytic mechanisms of cellular uptake nutraceuticals during nutrition therapy and cancer prevention.

1. Introduction

Nowadays, development of metallic nanoparticles such as gold and silver nanoparticles has successfully trapped the attentions and promised its effects and benefits on biosensing, bioimaging, and biomedical applications such as diseases therapeutics, diagnostics and drugs delivery [1–3]. Gold nanoparticles (AuNPs) is one of most investigated and popular metallic nanoparticles and have been well applied in imaging and carriers of drugs and/or biomolecules for diseases and cancers therapeutics in which are resulted from their easy fabrication process, tunable sizes, charges and unique physicochemical properties as well as easy functionalized with biomolecules, native nontoxic and biocompatibility [4,5]. Although the versatile benefits and advantages of AuNPs, several limitations such as penetration and/or permeability, drug retention, and vascular barriers are major problems in nanoparticles-based therapeutics and/or theranostics. Therefore, in order to improve the above defects and increase drug utilization, several ameliorating methods on nanoparticles such as surface chemistry modification with biopolymers and penetrated molecules to increase the cellular uptake ability, intracellular targeting and stability have been development [6,7].

Cells can “eat” and “drink” nutrients, proteins and biomolecules as well as microorganisms and/or cells from extracellular ambience through endocytic mechanisms, which have categorized into several types by based on the plasma membrane engulf morphologies and molecular features. These are including of phagocytosis, pinocytosis, circular dorsal ruffles and entosis [8]. In light of investigation on cellular uptake mechanisms of nanoparticles, most endocytosis mechanisms were emphasized on phagocytosis and pinocytosis. Phagocytosis can be evoked by cell undergoing microbials invasion, debris and/or particles which size larger than 500 nm. Further, pinocytosis is initiated by soluble and/or fluid substances and can be subclassified into clathrin-mediated endocytosis, caveolae-mediated endocytosis, clathrin- and caveolae-independent endocytosis as well as micropinocytosis [9,10]. Due to the widely application of nanoparticles such as AuNPs on biomedical and biotechnology [5], the cellular internalization of nanoparticles has been attracted the insight for understanding the endocytic mechanism so that improvement of nanoparticles-mediated drugs, antibodies, genes and biomolecules delivery efficiency.

As so far, exploiting nanomedicine through endocytosis has categorized into three groups including of phagocytosis, receptor-mediated endocytosis and subcellular region targeting *via*endocytic uptake and trafficking [11,12]. For examples, Wang et al. demonstrated that the drug-delivery system ANS-TAT-AuNP which modified AuNPs with a TAT, a potent cell membrane penetrating peptide and derived from the transcriptional activator of HIV-1, to enhance the anticancer molecule ANS-mediated the inhibition of cell proliferation and overcome the multidrug resistant of cancer cells [13]. Moreover, Saei et al. have summarized that controlled the nanoparticle surface chemistry through modified the surface charge, hydrophobicity and hydrophilicity could regulate the cellular uptake and the subcellular transport of NPs [14]. Accordingly, to understand and validate the differ nanoparticles-mediated endocytosis mechanisms will improve drug and/or biomolecules delivery efficacy, diseases and/or cancers therapeutics and disease theranostics.

Disease and/or cancer therapy and prevention using natural compounds and nutraceuticals for supporting convention therapy have attracted more and more attention which attributed to their promising of lower toxicity and decrease the side effects of conventional chemotherapy [15]. Avemar is fabricated from yeast-mediated fermentation of wheat germ extract and has been verified its efficacy benzoquinone components such as of 2-methoxy benzoquinone and 2, 6-dimethoxy benzoquinone (DMBQ) which were served as critical roles on anti-cancer, cancer prevention and nutrient therapy in *in vitro*, *in vivo* and human clinical trials [16–18]. Further, documents has proposed that Avemar could interfere cellular metabolisms such as inhibition of glucose uptake and nucleic acid synthesis, which involved in disturbed several enzyme activity in glycolysis and pentose phosphate pathway, to disrupt the tumor activity. These results are attributed to the high redox potential benzoquinone-derived components in Avemar [16]. By promising the safety and nontoxicity, Avemar has been widely used to be a nutraceutical for cancer prevention and nutritional therapy to enhance and supplement the conventional therapies [19]. Indeed, Avemar-mediated cell proliferation inhibition, cell apoptosis induction, cytotoxicity and cell cycle disturbing has systematically demonstrated in different types of cancer cells [20]. Although the mechanisms of Avemar-mediated anti-cancer activity and signaling transduction have well investigated and elucidated, the cellular uptake-mediated endocytic pathways still unclear.

In previous study, we have fabricated a biocompatible AuNP nanocarrier through conjugated AuNP with a biopolymer-collagen (AuNP-Col) and demonstrated their positively increase of cell proliferation and migration in MSCs and stimulation of the endothelial cell differentiation. In the present study, we further manufactured the AuNP-Collagen-Avemer (AuNP-Col-Ave) nanocarrier through incorporated Avemar into AuNP-Col nanocarrier. The AuNP-Col-Ave nanocarrier were next subjected to physicochemical properties analysis, detection of cell viability and validation of cellular uptake mechanisms in transformed SCC cells and non-transformed HSF and BAEC cell lines.

2. Materials and methods

2.1. Preparation of gold-collagen-Avemar nanocomposites (AuNP-Col-Ave) and FITC conjugation

The gold nanoparticle-collagen (AuNP-Col) has generated and described as the previous study [21,22]. No reference was found before published the novel method for preparation this AuNP-Col-Ave nanocarrier. Briefly, to prepare the AuNP-collagen-Avemar nanocarrier (AuNP-Col-Ave), the AuNP (Gold Nanotech Inc, Taiwan) was sonicated for 15 min and next thoroughly mixed with 100 µl of collagen (0.5 mg/ml, BD Bioscience, USA) in a 1:1 vol ratio at RT for 30 min and obtained the AuNP-Col nanocomposites with a volume of 200 µl (20 ppm). The AuNP-Col nanocomposites were further interacted with Avemar (0.5 mg/ml) in a 3:2 vol ratio at 4 °C for 2 h and obtained the AuNP-Col-Ave nanocomposites. For preparing a FITC conjugation, the AuNP-Col-Ave nanocomposites were generally interacted with FITC (0.5 mg/ml, Sigma) in a 50:1 vol ratio at 4 °C for 8 h. The generated AuNP-Col-Ave-FITC nanocomposites were further washed with deionized water for twice and kept in a dark at 4 °C.

2.2. Characterization

The fabricated AuNP-Col and AuNP-Col-Ave were further characterized their physical and chemical properties which have described as previously study [21]. Briefly, the UV–vis absorption spectrum was analyzed using UV–vis spectrophotometry (Helios Zeta, Thermo fisher Scientific Inc, USA) and the infrared (IR) spectra was obtained using a Fourier transform IR spectrometer (Shimadzu Pretige-21, Japan). Further, the hydrodynamic sizes were analyzed using Dynamic light

scattering (DLS, Zetasizer Nano Malwen ZS90, Taiwan). For zeta potential analysis, the fabricated AuNP-Col-Ave was pipetted into the disposable cuvette and the effective electric charge of the nanocarrier surface was evaluated using a DLS analyzer (ZETASIZER, Malvern ZS90, Taiwan) according to the manufacturer's instructions.

2.3. Cell culture

The transformed cells of oral squamous cell carcinoma SCC-4 cells were kindly provided by Prof. Da-Tian Bao [23] and were maintained in DMEM contained with 10% FBS, 2 mM glutamine, and 1% penicillin/streptomycin/neomycin. Non-transformed cells such as human skin fibroblasts (HSF) and bovine aortic endothelial cells (BAEC) were obtained from the American Type Cell Culture (ATCC) and maintained in low glucose Dulbecco's modified Eagle medium supplemented with 10% FBS and 1% (v/v) antibiotics (10,000 U/ml penicillin G and 10 mg/ml streptomycin). All the cells were maintained in a humidified atmosphere incubator with 5% CO_2 and 37 °C.

2.4. Cell viability assay

The cytotoxic effects of AuNP-Col-Ave were detected using a colorimetric MTT assay and Calcein AM Assay. Cells (1×10^4 cells/well) were seeded in 96 wells culture plate and then incubated with various doses of AuNP-Col-Ave (0.02, 0.04, 0.08, 0.16, 0.24, 0.48 and 0.96 mg/ml) for 48 h. Cells were then incubated with MTT agent (0.5 mg/ml) for 2 h at 37 °C and the further dissolved colorimetric formazan complex was analyzed at the absorption wavelength of 570 nm using an ELISA reader (SpectraMax M2, Molecular Devices, USA). The Calcein AM cell viability assay was executed according to the manufacturer's instructions. Briefly, after cells were treatment of AuNP-Col-Ave, cells were then incubated with Calcein AM solution (2 μM) in PBS for 30 min at 37 °C. the fluorescence images and fluorescence intensity were measured and recorded using a fluorescent microscopy (ZEISS AXIO Z1, USA) and Flow cytometer combined with FACS software (Becton Dickinson, USA), respectively.

2.5. Cellular uptake assay

Cells (1×10^5) were treated with AuNP-Col-Ave-FITC (0.5 mg/ml) for 2 h and washed away the excess nanoparticles with PBS. The cells were incubated for another 48 h at 37 °C. For fluorescence analysis, cells were washed with PBS and then subjected to 4% paraformaldehyde fixation, 0.5% Triton X-100 permeability and F-actin phalloidin staining (Rhodamine phalloidin, Sigma-Aldrich, USA) as well as DAPI nuclear staining (Invitrogen). The fluorescence images were obtained and carried out using a fluorescent microscopy (ZEISS AXIO Z1, USA). Moreover, the cellular uptake ability was further validated by detected the fluorescein-positive cells using flow cytometer and quantified with the FACS software (Becton Dickinson, USA). Next, to verify the cellular uptake mechanisms, cells (1×10^5) were pre-treated with several endocytosis inhibitors included Cytochalasin D (Cyto, 5 μM), Chlorpromazine (CPZ, 2 μM), Bafilomycin (Baf, 100 nM) and Methyl-β-cyclodextrin (β-MCD, 2.5 mM) for 1 h and then treated with AuNP-Col-

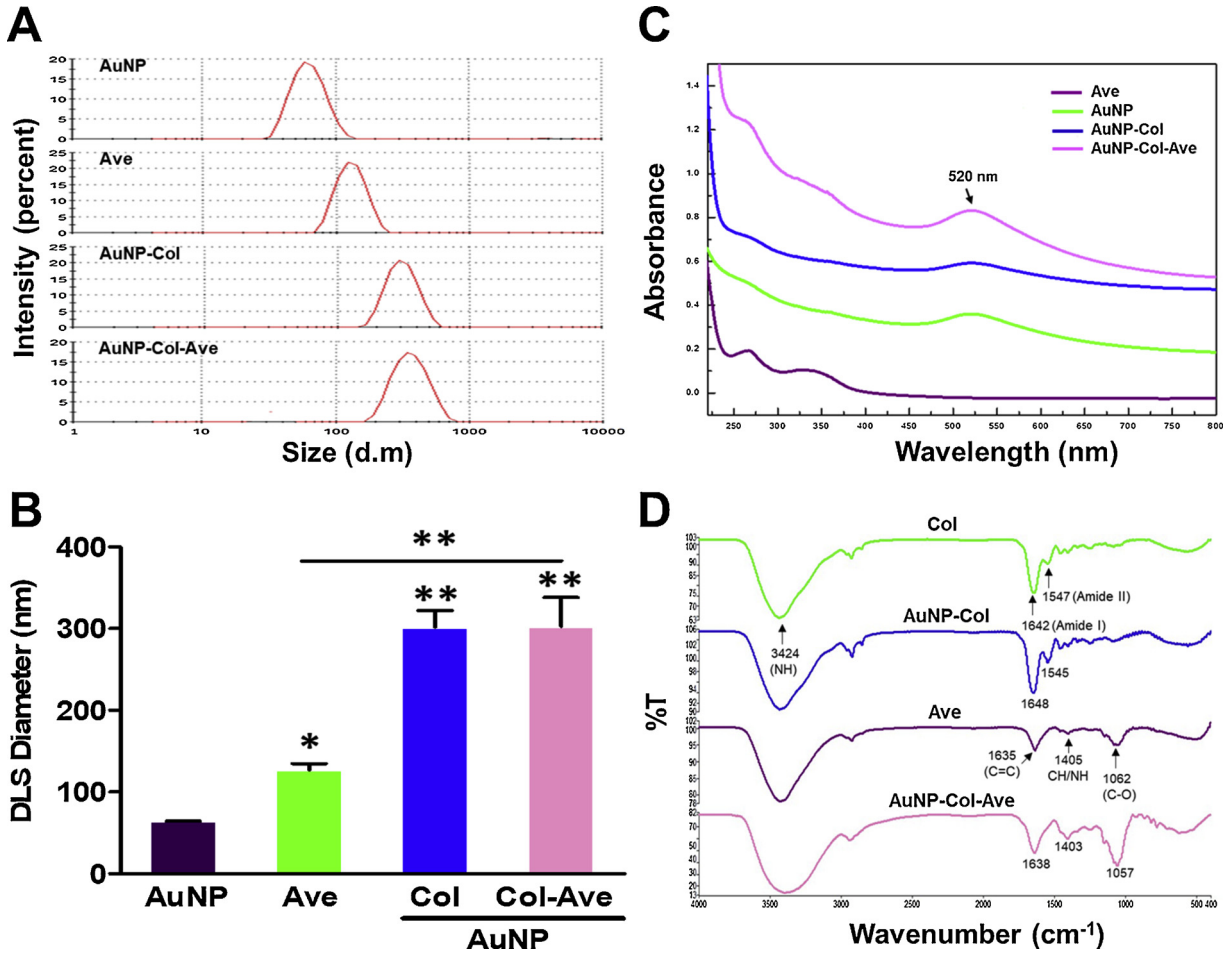

Fig. 1. Characterization of AuNP-derived nanocomposites: AuNP-Col and AuNP-Col-Ave. (A–B) The size distribution and quantification of AuNP-derived nanocarrier were determined respectively using DLS. (C). UV–Vis absorption spectra for AuNP-derived nanocomposites. (D) The FTIR spectra of Col, AuNP-Col, Ave and AuNP-Col-Ave nanocarrier in the total wavenumber ranges from 400 cm^{-1} to 4000 cm^{-1} regions. Data were presented as the mean ± SD (n = 3). $^{**}P < 0.05$, $^{**}P < 0.01$.

Ave-FITC (0.5 mg/ml) for 2 h. After cells were washed away the excess nanoparticles with PBS and incubated in culture medium for another 48 h at 37 °C, cells were subjected to fluorescence image assay and flow cytometry and the fluorescein positive cells were further quantified using the FACS software (Becton Dickinson, USA), respectively.

2.6. Statistical analysis

Data from multiple samples (n = 3–6) were collected for a given experiment and expressed as mean ± standard deviation. All experiments were independently repeated at least three times. Student's *t*-test and the single-factor analysis of variance (ANOVA) method were used to examine the difference between groups. For ANOVA, Bonferroni was chosen for post hoc analysis. The p values less than 0.05 ($p < 0.05$) were considered statistically significant.

3. Results and discussion

3.1. Characterization of the fabricated AuNP-collagen-Avemar (AuNP-Col-Ave) nanocomposites

We first characterized the physicochemical properties of AuNP-Col-Ave nanocarrier with dynamic light scattering (DLS), UV–vis absorption spectroscopy and IR spectra analysis (Fig. 1). The DLS assay revealed that the incorporated avemar would not affect the size distributions of AuNP-Col-Ave and has showed a similar size with AuNP-Col (Fig. 1A). The further quantification of size distributions was indicated that the average size of AuNP-Col-Ave is 303 ± 35.2 nm as comparing to 301.9 ± 20.4, 127 ± 7.7 and 64.2 ± 0.5 nm on AuNP-Col, Ave and AuNP, respectively (Fig. 1B). We also analyzed the zeta potential of AuNP-Col-Ave and obtained an effective surface electric charge of 43.6 ± 5.0 mV. Further, the UV–vis absorption data showed a peak was found at 520 nm on Ave conjugated AuNP-Col nanocarrier (Fig. 1C). The FTIR results of Col, AuNP-Col, native Ave, and AuNP-Col-Ave were represented in Fig. 1D. The peaks at 1547, 1642 and 3424 cm^{-1} of Col were indicated to the bands of amide II and amide I as well as NH stretching, respectively. Following AuNP incorporation, these two indicated amide peaks were shifted to lower frequency 1545 and higher frequency 1648 cm^{-1}, respectively. This result is corresponding to AuNP-conjugated with Col [22]. Moreover, the peaks of observed at 1062, 1405 and 1635 cm^{-1} on Ave were corresponded to the stretching of C–O [24], the coupled (C–H)/(NH–) plane-bending [25], and the aromatic C=C, respectively [26]. This may result from the chemical components of benzoquinone such as of 2-methoxy benzoquinone and 2, 6-dimethoxy benzoquinone (DMBQ) [18]. In AuNP-Col-Ave group, the peak of 1635 cm^{-1} which observed in native Ave was shifted into a higher frequency 1638 cm^{-1} and revealed a strong absorption. Further, the peaks of observed at 1405 and 1062 cm^{-1} of

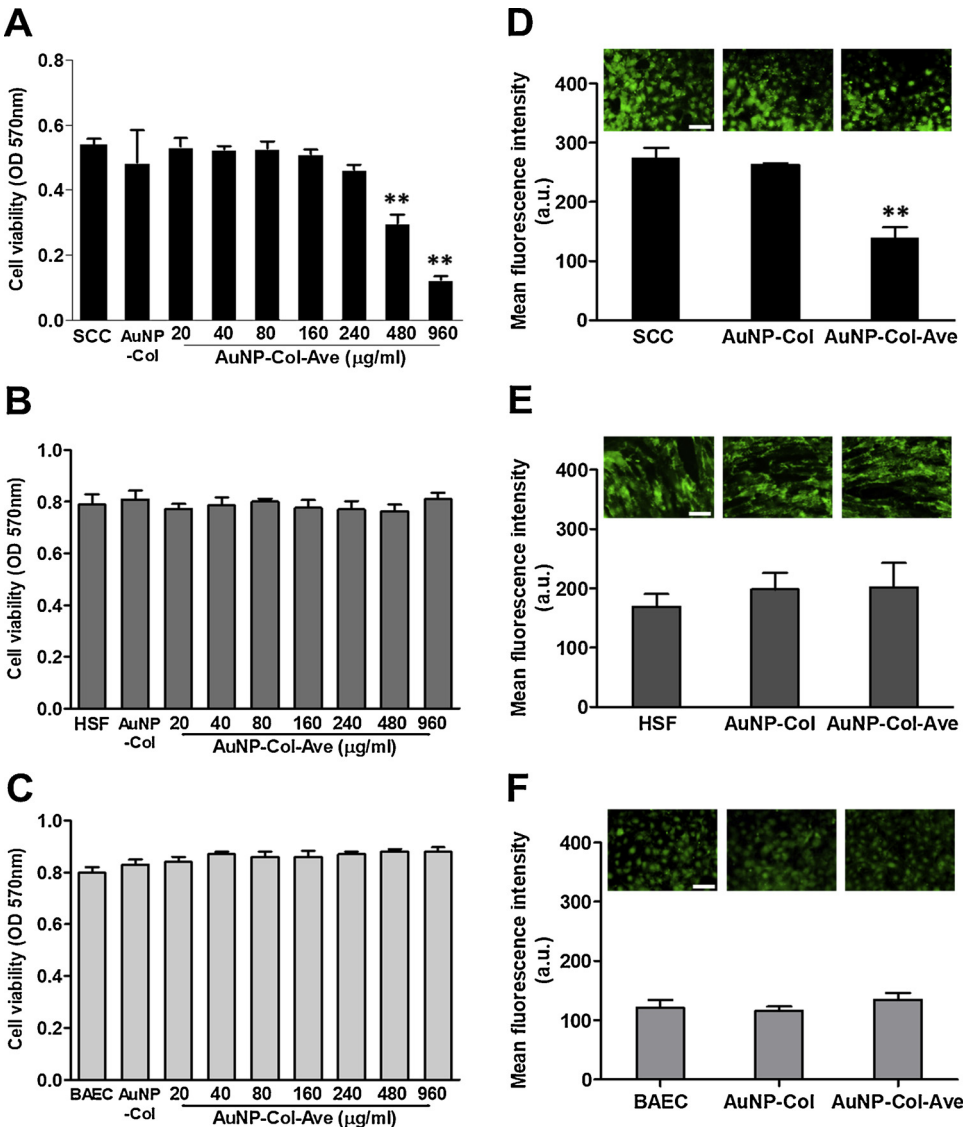

Fig. 2. Comparison of AuNP-Col-Ave-mediated on cell viability of transformed SCC cells and non-transformed HSF and BAEC cell lines using MTT assay and Calcein-AM staining assay. After Cells were treated with various doses of AuNP-Col-Ave for 48 h, a cytotoxicity effect was further validated using MTT assay (A–C). For further detected the effect of AuNP-Col-Ave on cell viability, cells were treated with AuNP-Col-Ave (500 μg/ml) for 48 h and then subjected to Calcein-AM staining assay. The data were next presented in fluorescence images and fluorescence intensity (D–F). Scale bars, 50 μm. Data were presented as the mean ± SD (n = 3). ** $P < 0.01$.

Ave were also shifted to lowering frequency with broad and absorption of 1403 and 1057 cm^{-1}, respectively. In addition, the peak of 1545 cm^{-1} which represented in AuNP-Col was disappearance followed Avemar incorporation. These results suggested that Ave is decorated onto AuNP-Col and formed into AuNP-Col-Ave nanocarrier. Altogether, these results indicated that the incorporation of Ave into AuNP-Col was achieved and obtained their average size about 303 nm.

3.2. The effects of AuNP-Col-Ave nanocarrier on cell viability and cytotoxicity of transformed oral cancer SCC cell line and non-transformed HSF and BAEC cell lines

So far, AuNP-based drug delivery, theranostics and therapeutics have been promised their enhancement of drug targeting release and elevation of diseases therapeutic efficacy including of cancers [27–29]. Here, we conjugated AuNP-Col with a natural multisubstance composition nutriments-Ave, which has been used clinically as a dietary supplement for malignant diseases [17], and investigated the effects of the fabricated AuNP-Col-Ave on cytotoxicity and cell viability of transformed and non-transformed cell lines, respectively. By MTT assay, AuNP-Col-Ave induced a significant cytotoxicity (˜50%) on transformed SCC cells rather than non-transformed HSF and BAEC cell lines at an administrated dose of 480 μg/ml (Fig. 2A–C). The IC50 value of AuNP-Col-Ave was further obtained at 620 μg/ml in SCC cells. To further validate the effect of AuNP-Col-Ave on cell viability, these cell lines were subjected to Calcein-AM staining assay. Our result revealed that SCC cells were more susceptible for AuNP-Col-Ave administration as compared to non-transformed HSF and BAEC cell lines (Fig. 2D–F). Additionally, the friendly and no toxic effects of AuNP-Col-Ave on these non-transformed HSF and BAEC cell lines have been further verified using FACS analysis and results showed that AuNP-Col-Ave treatment neither change cell cycle distribution nor induce cell apoptosis (Figs. S1 and S2). These data suggested that AuNP-Col-Ave significantly induced a cytotoxicity on transformed cells as compared to non-transformed cells.

Gold nanoparticle grafted biopolymers including of collagen, polyurethane and fibronectin have been demonstrated the potent biomedical applications in activation of cellular behaviors such as cell migration, cell adhesion and cell growth in endothelial cells and fibroblast cells, and induction of cell differentiation and vascular regeneration in mesenchymal stem cells [21,30–32]. In addition, based on the AuNP photochemical properties, AuNP-collagen nanocarrier also displayed their excellent efficacy of anti-tumorigenicity in *in vivo* through the photothermal and/or photodynamic fashions [33,34]. Accordingly, the AuNP-conjugated biopolymers, have been promised their excellent bioactivity, biomimetic interface and biocompatibility, which were

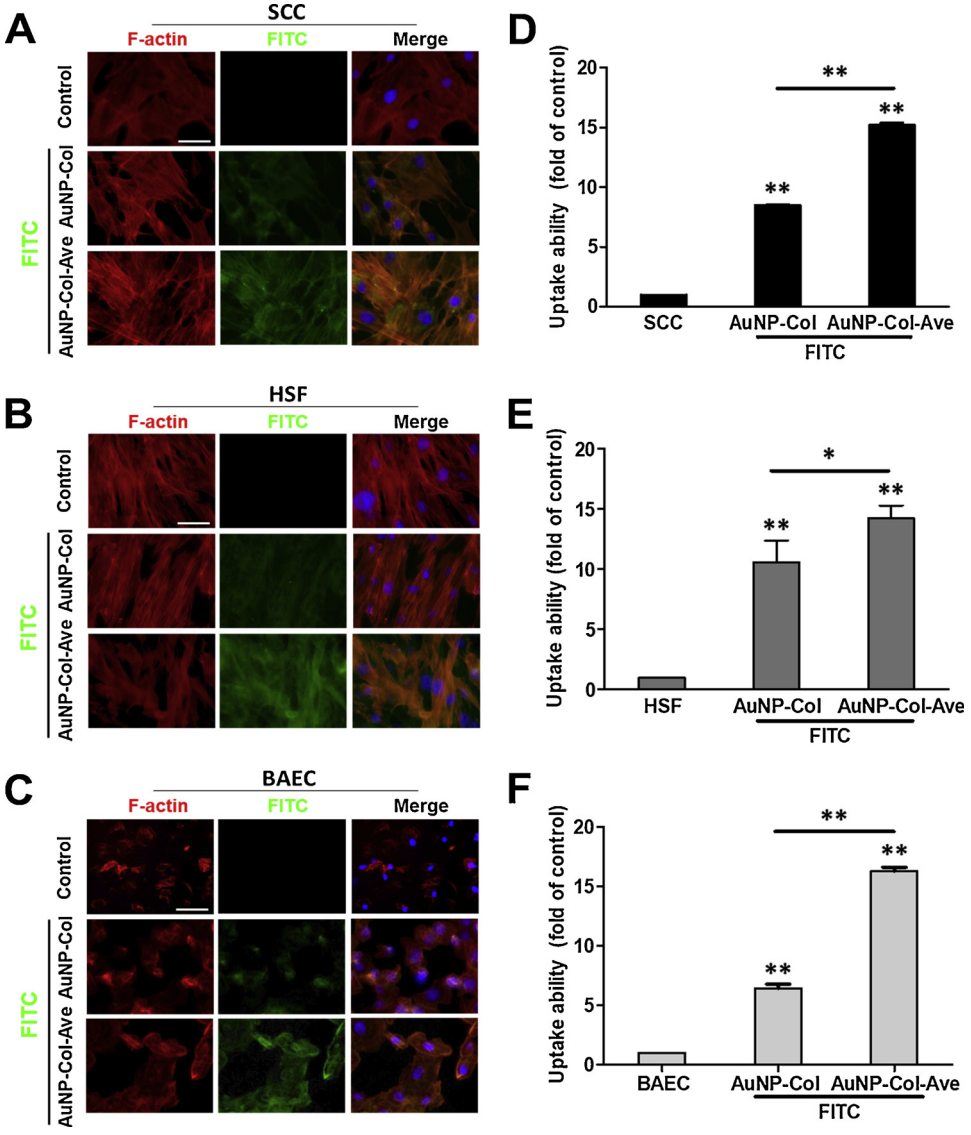

Fig. 3. Evaluation of Cellular uptake ability on FITC conjugated with AuNP-Col and/or AuNP-Col-Ave in transformed and non-transformed cell lines, respectively. After cells were treated with AuNP-Col-FITC and/or AuNP-Col-Ave (500 μg/ml) for 2 h and then incubated for another 48 h, cells were subjected to F-actin phalloidin staining and detected the cellular uptake ability using fluorescence microscopy and FACS analysis, respectively. (A–C) The uptake efficiency of both AuNP-Col and AuNP-Col-Ave was analyzed on the transformed SCC cells and non-transformed HSF and BAEC cells using fluorescence microscopy. (D–F) the uptake efficiency of both AuNP-Col and AuNP-Col-Ave on these cell lines were further assessed and quantified using FACS analysis. Scale bars, 50 μm. Data were presented as the mean ± SD (n = 3). *$P <$ 0.05, ** $P <$ 0.01.

regarded as good candidates for carrier of compounds and/or drugs. Avemar is a nontoxic wheat germ extract and biocompatible nutriment and has wildly used as an ingredient in dietary supplements for cancer patients [35]. Moreover, Ave-mediated cytotoxicity has been demonstrated in many types of cancers such as colon cancer, head and neck cancer, breast cancer and ovary cancer in *in vivo* and *in vitro* [35,36]. In this study, we showed the AuNP-Col-Ave selectively induced cytotoxicity in oral cancer SCC cells and revealed biocompatibility in non-transformed HSF and BAEC cell lines. Due to highly glucose consumption and glucose metabolism are necessary for tumor cell proliferation and tumor growth. Avemar can serve as an antagonist for inhibition of glucose uptake and interfering enzymes functions which involved in anaerobic glycolysis and PPP (pentose phosphate pathway) glucose metabolism as well as disruption of DNA and RNA synthesis [37,38]. Therefore, these reports may explain why Ave is more friendly and/or biocompatibility for normal and/or non-transformed cells rather than tumor cells. In addition, previous study has indicated that Ave significantly inhibited cell viability in oral cancer SCC cells and obtained the IC 50 value of 980 μg/ml at 48 h [23]. While in the present study, AuNP-Col-Ave revealed a dramatical decrease of IC 50 value (620 μg/ml) in the SCC cells. This result suggested that AuNP-Col as an ideal carrier and thus enhancing uptake efficacy, cytotoxicity and biofunction of Ave in cancerous SCC cells.

3.3. The fabricated AuNP-Col-Ave nanocarrier enhance cellular uptake capacity

A highly delivery efficiency of drug, gene and /or biomolecules into target cells is crucial step for infectious diseases control, cancer therapeutics and/or theranostics. Endocytosis is important mechanisms for cells processing their taken up of nutrients, growth factors, biomolecules and drugs from the environment as well as recycling the cell apoptotic debris and eliminating the pathogens from the ambiences [39]. Here, to understand the AuNP-Col-Ave-mediated different cell fates on transformed and non-transformed cell lines, we next examined the cellular internalized capacity for AuNP-Col-Ave in these cell lines using fluorescence measurement assay and FACS analysis. We first conjugated AuNP-Col-Ave with FITC (AuNP-Col-Ave-FITC) and then incubated these cell lines with the nanocomposites for 2 h. After cells were incubated for another 48 h, the cellular uptake capacity for AuNP-Col-Ave-FITC was verified using fluorescence measurement. As shown in Fig. 3, fluorescent image assay indicated that AuNP-Col-Ave reveals an excellent internalized ability as compared to AuNP-Col in these three cell types (Fig. 3A–C). Moreover, FACS analysis also revealed that Ave incorporation is dramatically enhancing AuNP-Col internalization in these cell lines (Fig. 3D–F). These results suggested that AuNP-Col-Ave could induce a significant uptake capacity as compared to AuNP-Col in

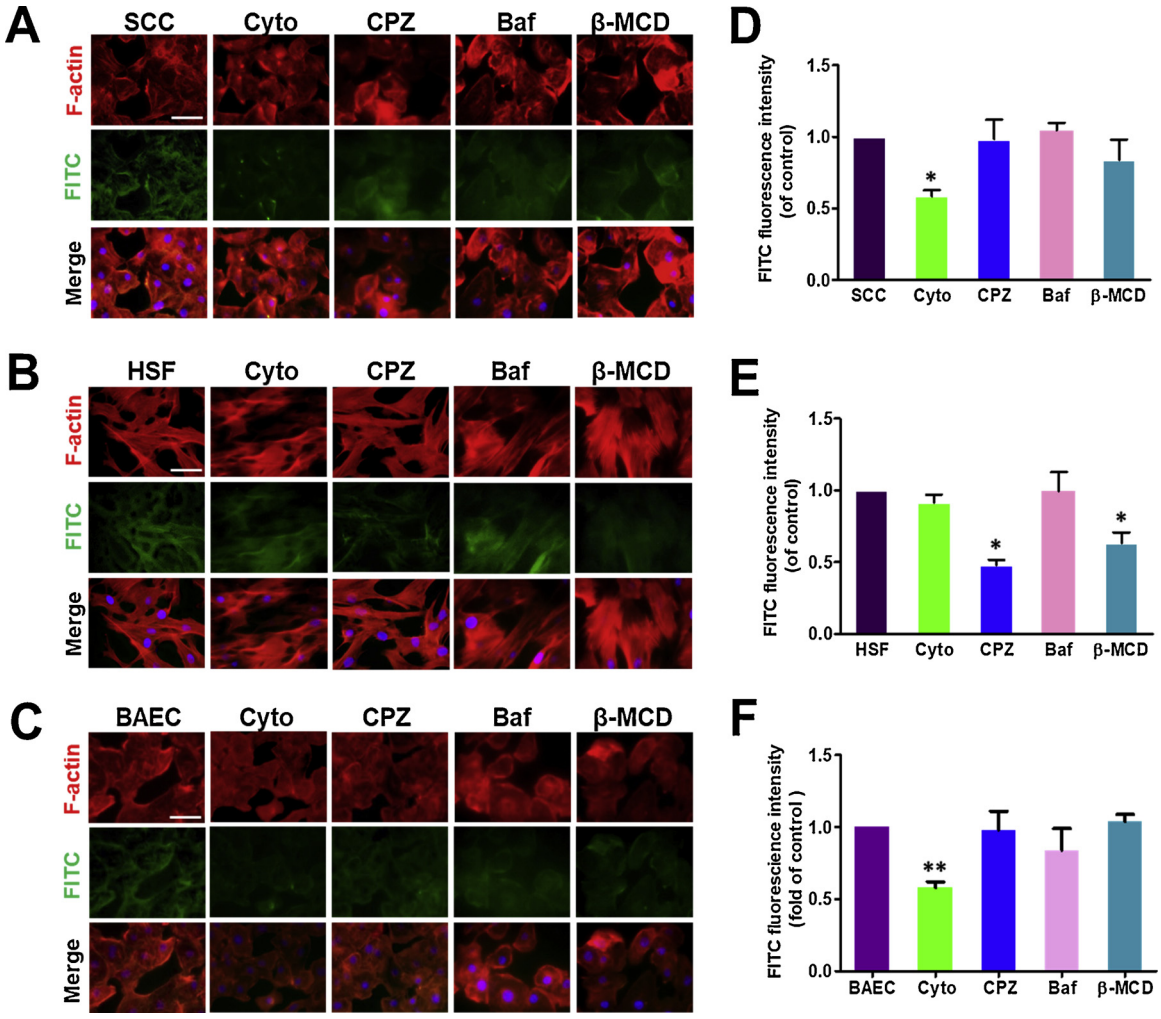

Fig. 4. Determination of AuNP-Col-Ave-mediated cellular uptake mechanisms. Cells (included the transformed SCC cells and non-transformed HSF and BAEC cells) were pre-treated with several endocytosis inhibitors included Cytochalasin D (Cyto), Chlorpromazine (CPZ), Bafilomycin (Baf) and Methyl-β-cyclodextrin (β-MCD) for 1 h and then incubated with AuNP-Col-Ave-FITC (500 μg/ml) for 2 h. Cells were next subjected to fluorescence image assay (A–C) and flow cytometry (D–F) and the fluorescein positive cells were further quantified using the FACS software (Becton Dickinson, USA), respectively. Scale bar, 50 μm. Data were presented as the mean ± SD (n = 3). *$P < 0.05$, ** $P < 0.01$.

both transformed and non-transformed cell types.

3.4. Determination of the cellular uptake mechanisms of AuNP-Col-Ave nanocarrier

Endocytosis is predominantly categorized into phagocytosis, endocytosis and macropinocytosis. Moreover, triggering of different endocytic mechanisms is highly associated with the physicochemical properties of nanoparticles such as size, shape, surface charge and surface chemical properties [9,10]. Due to the AuNP-Col-Ave induce the excellent cellular uptake and trigger different viability fates within these transformed and non-transformed cell lines, we next validated the AuNP-Col-Ave -mediated cellular uptake mechanisms in these cell lines. Here, several pharmacological inhibitors included Cytochalasin D (Cyto), Chlorpromazine (CPZ), Bafilomycin (Baf) and Methyl-β-cyclodextrin (β-MCD) were used to investigate which endocytic pathways were involved in AuNP-Col-Ave internalization. Where the Cyto is an inhibitor for actin polymerization and have been suggested that disturbed macropinocytosis [40], CPZ is involved in the inhibition of Rho GTPase-mediated clathrin-mediated endocytosis (CME) [41], Baf is known a vacuolar ATPase inhibitor which involved in an interfering of cell autophagy [42,43], and β-MCD is a cholesterol captor and may perturb membrane lipid raft associated endocytic pathway such as micropinocytosis, clathrin-mediated endocytosis and clathrin-independent endocytosis (CIE) [9,44]. In this study, cells were first pre-treated with endocytosis inhibitors for 1 h, and then incubated with AuNP-Col-Ave-FITC for another 2 h. Cells were subsequently harvested and subjected to analyze the uptake mechanisms of AuNP-Col-Ave. By using fluorescence image analysis, the internalization of AuNP-Col-Ave was obviously inhibited by Cyto treatment as compared to other inhibitors in cancerous SSC cells (Fig. 4A). For non-transformed HSF cells, we found that both inhibitors of CPZ and β-MCD were significantly interfered the internalization of AuNP-Col-Ave (Fig. 4B). Interestingly, the Cyto disturbed AuNP-Col-Ave internalization was also found in non-transformed BAEC cells (Fig. 4C). Moreover, the consistently results were also found in FACS analysis (Fig. 4D–F). These results suggested that AuNP-Col-Ave internalization in cancerous SCC cells and bovine aortic endothelial BAEC cells were through the macropinocytosis. Moreover, several mechanisms including of micropinocytosis, clathrin-mediated endocytosis and clathrin-independent endocytosis were involved in AuNP-Col-Ave internalization on fibroblast HSF cells.

Based on there are different subcategorized mechanisms involved in endocytosis, many methodologies have been well developed and widely used to investigate cellular uptake mechanism such as inhibitors, mutated proteins by gene manipulation and siRNA introduction [9]. Moreover, the nanoparticle sizes were always one of important factors during investigation of cellular uptake mechanisms [45]. Indeed, previous study indicated that cell allowed the nanoparticles entering into vesicles with a size range of 10–1000 nm, in which the large particles (200–500 nm) were internalized may through macropinocytosis. The

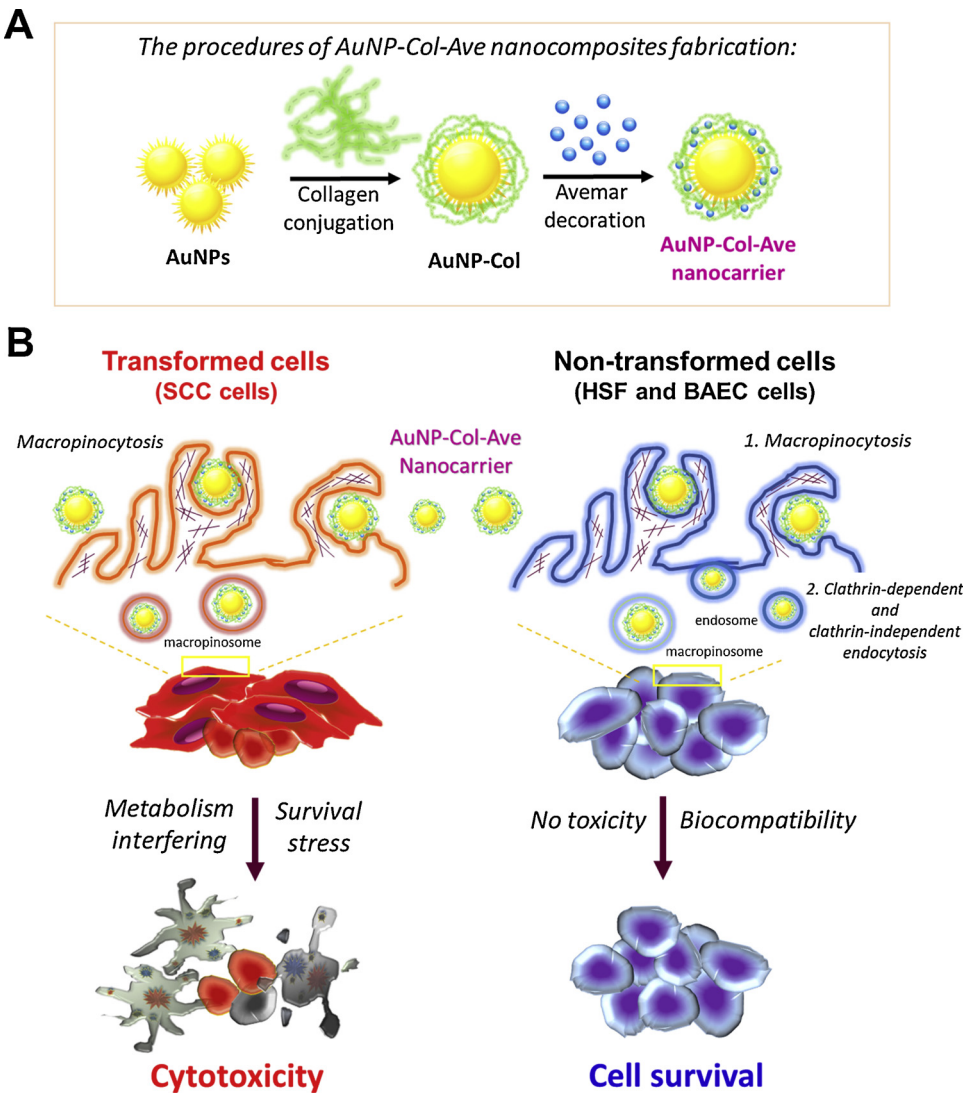

Fig. 5. Schematic diagram illustrated that AuNP-Col-Ave-mediated cellular uptake mechanisms and cell fates in both transform and non-transformed cell lines. (A) The procedures for AuNP-Col-Ave fabrication. (B) The biofunctional assays of AuNP-Col-Ave were executed in transformed and non-transformed cell lines in which included of cell viability and cellular uptake mechanism. We showed that AuNP-Col-Ave-induced a significant cytotoxicity in cancerous SCC cells and exhibited non-toxicity and biocompatibility for non-transformed BAEC and HFS cells. This result indicated that the different survival stress may be attributed to Avemar-mediated a metabolism disturbing in transformed cells rather than non-transformed cells. Moreover, cellular uptake mechanisms of AuNP-Col-Ave were revealed that macropinocytosis pathway is adapted in all three cell types. Moreover, the additional clathrin-dependent and clathrin-independent endocytosis were exclusively found in non-transformed HSF cells.

particles sizes around 10–300 nm and 60–80 nm would be involved in clathrin-mediated endocytosis and caveolae-mediated endocytosis, respectively. In addition, the other clathrin-independent pathway may be responsible for particles size lower 100 nm [39,46,47]. In addition, the positively charged AuNP-Col-Ave (43.6 ± 5.0 mV) may also play an important role for cellular uptake due to their easily attracted and bound to the negatively charged cell membrane surface which could elicit a endocytic mechanism of macropinocytosis [10].

In this study, we detected the stature of Ave-incorporated AuNP-Col nanocarrier and obtained an average particle size of 303 nm. Moreover, we found that the macropinocytosis seems to be the favorite endocytic mechanism during AuNP-Col-Ave internalized into these transformed and non-transformed cell lines. Although macropinocytosis was utilized in both SCC cells and BAEC cells during AuNP-Col-Ave treatment, the cellular fates between SCC cells and BAEC cells were remained different (Fig. 2). Moreover, our data also implied that AuNP-Col-Ave-mediated endocytic pathways were adopted in a cell types-dependent manner. Therefore, to further understand the AuNP-Col-Ave-mediated endocytic mechanisms, thoroughly validation of the cellular uptake-mediated signaling pathways is guaranteed and necessary in the future.

4. Conclusion

In this study, we first deposited the fermented extract of wheat germ called Avemar into AuNP-collagen nanocarrier (AuNP-Col-Ave) and methodologically detected their physicochemical properties and biological effects on transformed SCC cells and non-transformed BAEC and HSF cells. Our results showed that AuNP-Col-Ave own an average particle size of 303 nm and revealed a significant cytotoxicity in cancerous SCC cells as well as exhibited nontoxicity and biocompatibility for non-transformed BAEC and HFS cells. Further, AuNP-Col-Ave nanocarrier also validated the excellent cellular uptake capacity as compared to AuNP-Col nanocarrier. Interestingly, the uptake mechanisms analysis revealed that macropinocytosis pathway is the major mechanism utilized for AuNP-Col-Ave internalization in these cell types. Moreover, the additional clathrin-dependent and clathrin-independent endocytosis were exclusively found in non-transformed HSF cells (Fig. 5). Altogether, this study is first validating the endocytic mechanisms of AuNP-Col-Ave nanocarrier in transformed and non-transformed cell lines. Our findings will provide a novel insight for endocytic mechanisms of cellular uptake nutraceuticals during nutrition therapy and cancer prevention.

Declaration of Competing Interest

The authors have declared that no competing interest exists.

Acknowledgements

This work was supported by the Ministry of Science and Technology of Taiwan (MOST 106-2321-B-110 -001-MY3and China Medical University Hospital, Taiwan (DMR-106-077).

Appendix A. Supplementary data

Supplementary material related to this article can be found, in the online version, at doi:https://doi.org/10.1016/j.colsurfa.2019.123791.

References

[1] P.K. Jain, X. Huang, I.H. El-Sayed, M.A. El-Sayed, Noble metals on the nanoscale: optical and photothermal properties and some applications in imaging, sensing, biology, and medicine, Acc. Chem. Res. 41 (2008) 1578–1586.
[2] Y. Yu, B.Y. Mok, X.J. Loh, Y.N. Tan, Rational design of biomolecular templates for synthesizing multifunctional noble metal nanoclusters toward personalized theranostic applications, Adv. Healthc. Mater. 5 (2016) 1844–1859.
[3] Q. Zhang, M. Yang, Y. Zhu, C. Mao, Metallic nanoclusters for cancer imaging and therapy, Curr. Med. Chem. 25 (2018) 1379–1396.
[4] F.-Y. Kong, J.-W. Zhang, R.-F. Li, Z.-X. Wang, W.-J. Wang, W. Wang, Unique roles of gold nanoparticles in drug delivery, targeting and imaging applications, Molecules 22 (2017).
[5] N. Elahi, M. Kamali, M.H. Baghersad, Recent biomedical applications of gold nanoparticles: a review, Talanta 184 (2018) 537–556.
[6] J.K. Patra, G. Das, L.F. Fraceto, E.V.R. Campos, M. Rodriguez-Torres, L.S. Acosta-Torres, L.A. Diaz-Torres, R. Grillo, M.K. Swamy, S. Sharma, S. Habtemariam, H.-S. Shin, Nano based drug delivery systems: recent developments and future prospects, J. Nanobiotechnol. 16 (2018) 71.
[7] A. Kumar, X. Zhang, X.-J. Liang, Gold nanoparticles: emerging paradigm for targeted drug delivery system, Biotechnol. Adv. 31 (2013) 593–606.
[8] G.J. Doherty, H.T. McMahon, Mechanisms of endocytosis, Annu. Rev. Biochem. 78 (2009) 857–902.
[9] T.-G. Iversen, T. Skotland, K. Sandvig, Endocytosis and intracellular transport of nanoparticles: present knowledge and need for future studies, Nano Today 6 (2011) 176–185.
[10] P. Foroozandeh, A.A. Aziz, Insight into cellular uptake and intracellular trafficking of nanoparticles, Nanoscale Res. Lett. 13 (2018) 339.
[11] A. Akinc, G. Battaglia, Exploiting endocytosis for nanomedicines, Cold Spring Harb. Perspect. Biol. 5 (2013) a016980.
[12] J. Kim, Y.M. Lee, Y. Kang, W.J. Kim, Tumor-homing, size-tunable clustered nanoparticles for anticancer therapeutics, ACS Nano 8 (2014) 9358–9367.
[13] R.-H. Wang, J. Bai, J. Deng, C.-J. Fang, X. Chen, TAT-modified gold nanoparticle carrier with enhanced anticancer activity and size effect on overcoming multidrug resistance, ACS Appl. Mater. Interfaces 9 (2017) 5828–5837.
[14] A.A. Saei, M. Yazdani, S.E. Lohse, Z. Bakhtiary, V. Serpooshan, M. Ghavami, M. Asadian, S. Mashaghi, E.C. Dreaden, A. Mashaghi, M. Mahmoudi, Nanoparticle surface functionality dictates cellular and systemic toxicity, Chem. Mater. 29 (2017) 6578–6595.
[15] S. Nobili, D. Lippi, E. Witort, M. Donnini, L. Bausi, E. Mini, S. Capaccioli, Natural compounds for cancer treatment and prevention, Pharmacol. Res. 59 (2009) 365–378.
[16] G.L. Johanning, F. Wang-Johanning, Efficacy of a medical nutriment in the treatment of cancer, Altern. Ther. Health Med. 13 (2007) 56–63.
[17] T. Mueller, W. Voigt, Fermented wheat germ extract–nutritional supplement or anticancer drug? Nutr. J. 10 (2011) 89.
[18] D.J. Cosgrove, D.G. Daniels, E.N. Greer, J.B. Hutchinson, T. Moran, F.K. Whitehead, Isolation of methoxy- and 2:6-dimethoxy-p-benzoquinone from fermented wheat germ, Nature 169 (1952) 966–967.
[19] J.T. Heimbach, G. Sebestyen, G. Semjen, E. Kennepohl, Safety studies regarding a standardized extract of fermented wheat germ, Int. J. Toxicol. 26 (2007) 253–259.
[20] K. Zhurakivska, G. Troiano, V.C.A. Caponio, M. Dioguardi, C. Arena, L. Lo Muzio, The effects of adjuvant fermented wheat germ extract on cancer cell lines: a systematic review, Nutrients 10 (2018).
[21] H.S. Hung, C.H. Chang, C.J. Chang, C.M. Tang, W.C. Kao, S.Z. Lin, H.H. Hsieh, M.Y. Chu, W.S. Sun, S.H. Hsu, In vitro study of a novel nanogold-collagen composite to enhance the mesenchymal stem cell behavior for vascular regeneration, PLoS One 9 (2014) e104019.
[22] S.C. Hsieh, H.J. Chen, S.H. Hsu, Y.C. Yang, C.M. Tang, M.Y. Chu, P.Y. Lin, R.H. Fu, M.L. Kung, Y.W. Chen, B.W. Yeh, H.S. Hung, Prominent vascularization capacity of mesenchymal stem cells in collagen-gold nanocomposites, ACS Appl. Mater. Interfaces 8 (2016) 28982–29000.
[23] M.D. Yang, W.S. Chang, C.W. Tsai, M.F. Wang, Y.C. Chan, K.C. Chan, M.C. Lu, A.W. Kao, C.M. Hsu, D.T. Bau, Inhibitory effects of AVEMAR on proliferation and metastasis of oral cancer cells, Nutr. Cancer 68 (2016) 473–480.
[24] V. Badalamoole, S. Abubakar Zauro, Absorptive removal of Cu2+ and Pb2+ from aqueous solutions using xanthan gum-g-poly[(N,N′-dimethylacrylamide)-co-(2-acrylamido-2-methylpropanesulfonic acid)]–ZnO nanocomposite gel, Sep. Sci. Technol. 54 (2019) 2164–2179.
[25] M. Strickland, O. Juárez, Y. Neehaul, D.A. Cook, B. Barquera, P. Hellwig, The conformational changes induced by ubiquinone binding in the Na+-pumping NADH:ubiquinone oxidoreductase (Na+-NQR) are kinetically controlled by conserved glycines 140 and 141 of the NqrB subunit, J. Biol. Chem. 289 (2014) 23723–23733.
[26] J. Fu, W. Liu, Z. Hao, X. Wu, J. Yin, A. Panjiyar, X. Liu, J. Shen, H. Wang, Characterization of a low shrinkage dental composite containing bismethylene spiroorthocarbonate expanding monomer, Int. J. Mol. Sci. 15 (2014) 2400–2412.
[27] N.S. Elbialy, M.M. Fathy, W.M. Khalil, Doxorubicin loaded magnetic gold nanoparticles for in vivo targeted drug delivery, Int. J. Pharm. 490 (2015) 190–199.
[28] J.R. Nicol, D. Dixon, J.A. Coulter, Gold nanoparticle surface functionalization: a necessary requirement in the development of novel nanotherapeutics, Nanomedicine (Lond) 10 (2015) 1315–1326.
[29] B. Panchapakesan, B. Book-Newell, P. Sethu, M. Rao, J. Irudayaraj, Gold nanoprobes for theranostics, Nanomedicine (Lond) 6 (2011) 1787–1811.
[30] H.S. Hung, M.Y. Chu, C.H. Lin, C.C. Wu, S.H. Hsu, Mediation of the migration of endothelial cells and fibroblasts on polyurethane nanocomposites by the activation of integrin-focal adhesion kinase signaling, J. Biomed. Mater. Res. A. 100 (2012) 26–37.
[31] Y.W. Chen, S.C. Hsieh, Y.C. Yang, S.H. Hsu, M.L. Kung, P.Y. Lin, H.H. Hsieh, C.H. Lin, C.M. Tang, H.S. Hung, Functional engineered mesenchymal stem cells with fibronectin-gold composite coated catheters for vascular tissue regeneration, Nanomedicine 14 (2018) 699–711.
[32] R. Xing, T. Jiao, L. Yan, G. Ma, L. Liu, L. Dai, J. Li, H. Möhwald, X. Yan, Colloidal gold–collagen protein core–shell nanoconjugate: one-step biomimetic synthesis, layer-by-layer assembled film, and controlled cell growth, ACS Appl. Mater.

Interfaces 7 (2015) 24733–24740.
[33] R. Xing, K. Liu, T. Jiao, N. Zhang, K. Ma, R. Zhang, Q. Zou, G. Ma, X. Yan, An injectable self-assembling collagen-gold hybrid hydrogel for combinatorial antitumor photothermal/photodynamic therapy, Adv. Mater. 28 (2016) 3669–3676.
[34] J. Sun, Y. Guo, R. Xing, T. Jiao, Q. Zou, X. Yan, Synergistic in vivo photodynamic and photothermal antitumor therapy based on collagen-gold hybrid hydrogels with inclusion of photosensitive drugs, Colloids Surf. A Physicochem. Eng. Asp. 514 (2017) 155–160.
[35] A. Telekes, M. Hegedus, C.H. Chae, K. Vekey, Avemar (wheat germ extract) in cancer prevention and treatment, Nutr. Cancer 61 (2009) 891–899.
[36] T. Mueller, K. Jordan, W. Voigt, Promising cytotoxic activity profile of fermented wheat germ extract (Avemar®) in human cancer cell lines, J. Exp. Clin. Cancer Res. 30 (2011) 42.
[37] L.G. Boros, K. Lapis, B. Szende, R. Tomoskozi-Farkas, A. Balogh, J. Boren, S. Marin, M. Cascante, M. Hidvegi, Wheat germ extract decreases glucose uptake and RNA ribose formation but increases fatty acid synthesis in MIA pancreatic adenocarcinoma cells, Pancreas 23 (2001) 141–147.
[38] B. Comin-Anduix, L.G. Boros, S. Marin, J. Boren, C. Callol-Massot, J.J. Centelles, J.L. Torres, N. Agell, S. Bassilian, M. Cascante, Fermented wheat germ extract inhibits glycolysis/pentose cycle enzymes and induces apoptosis through poly(ADP-ribose) polymerase activation in Jurkat T-cell leukemia tumor cells, J. Biol. Chem. 277 (2002) 46408–46414.
[39] M. Bohdanowicz, S. Grinstein, Role of phospholipids in endocytosis, phagocytosis, and macropinocytosis, Physiol. Rev. 93 (2013) 69–106.
[40] R. Kanlaya, K. Sintiprungrat, S. Chaiyarit, V. Thongboonkerd, Macropinocytosis is the major mechanism for endocytosis of calcium oxalate crystals into renal tubular cells, Cell Biochem. Biophys. 67 (2013) 1171–1179.
[41] L.H. Wang, K.G. Rothberg, R.G. Anderson, Mis-assembly of clathrin lattices on endosomes reveals a regulatory switch for coated pit formation, J. Cell Biol. 123 (1993) 1107–1117.
[42] J. Xu, H.T. Feng, C. Wang, K.H.M. Yip, N. Pavlos, J.M. Papadimitriou, D. Wood, M.H. Zheng, Effects of Bafilomycin A1: an inhibitor of vacuolar H (+)-ATPases on endocytosis and apoptosis in RAW cells and RAW cell-derived osteoclasts, J. Cell. Biochem. 88 (2003) 1256–1264.
[43] C. Mauvezin, T.P. Neufeld, Bafilomycin A1 disrupts autophagic flux by inhibiting both V-ATPase-dependent acidification and Ca-P60A/SERCA-dependent autophagosome-lysosome fusion, Autophagy 11 (2015) 1437–1438.
[44] D. Dutta, J.G. Donaldson, Search for inhibitors of endocytosis: intended specificity and unintended consequences, Cell. Logist. 2 (2012) 203–208.
[45] S. Zhang, J. Li, G. Lykotrafitis, G. Bao, S. Suresh, Size-dependent endocytosis of nanoparticles, Adv. Mater. 21 (2009) 419–424.
[46] L. Kou, J. Sun, Y. Zhai, Z. He, The endocytosis and intracellular fate of nanomedicines: implication for rational design, Asian J. Pharm. Sci. 8 (2013) 1–10.
[47] B. Kang, M.M. Afifi, L.A. Austin, M.A. El-Sayed, Exploiting the nanoparticle plasmon effect: observing drug delivery dynamics in single cells via Raman/fluorescence imaging spectroscopy, ACS Nano 7 (2013) 7420–7427.